Journal Pre-proofs

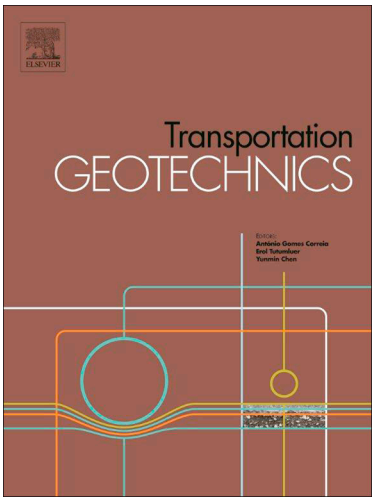

PERFORMANCE OF CALCIUM LIGNOSULFONATE AS A STABILISER OF HIGHLY EXPANSIVE CLAY

Mariano T. Fernandez, Sandra Orlandi, Mauro Codevilla, Teresa M. Piqué, Diego Manzanal

PII: S2214-3912(20)30357-3
DOI: https://doi.org/10.1016/j.trgeo.2020.100469
Reference: TRGEO 100469

To appear in: *Transportation Geotechnics*

Received Date: 4 December 2019
Revised Date: 5 October 2020
Accepted Date: 1 November 2020

Please cite this article as: M.T. Fernandez, S. Orlandi, M. Codevilla, T.M. Piqué, D. Manzanal, PERFORMANCE OF CALCIUM LIGNOSULFONATE AS A STABILISER OF HIGHLY EXPANSIVE CLAY, *Transportation Geotechnics* (2020), doi: https://doi.org/10.1016/j.trgeo.2020.100469

PERFORMANCE OF CALCIUM LIGNOSULFONATE AS A STABILISER OF HIGHLY EXPANSIVE CLAY

Mariano T. Fernandez[1,2], Sandra Orlandi [3], Mauro Codevilla[1,2], Teresa M. Piqué[2,3], Diego Manzanal[1,4,5] *

[1] *Instituto de Tecnología y Ciencias de la Ingeniería (INTECIN), Universidad de Buenos Aires (UBA), CONICET, Facultad de Ingeniería, LAME, Av. Las Heras 2214, 1426, Buenos Aires, Argentina.*
[2] *Instituto de Tecnología en Polímeros y Nanotecnología (ITPN UBA- CONICET) Av. Las Heras 2214, 1426, Buenos Aires, Argentina, Av. Las Heras 2214, Buenos Aires, Argentina*
[3] *Universidad de Buenos Aires (UBA), Facultad de Ingeniería, LAME, Av. Las Heras 2214, 1426, Buenos Aires, Argentina, Av. Las Heras 2214, Buenos Aires, Argentina*
[4] *Universidad Nacional de la Patagonia, Facultad de Ingeniería, Dpto. Ingeniería Civil, RP Nº1 km4, Ciudad Universitaria, 9005, Comodoro Rivadavia, Argentina*
[5] *ETS de Ingenieros de Caminos, Canales y Puertos, Universidad Politécnica de Madrid, c/ Prof. Aranguren 3, Ciudad Universitaria, 28040, Madrid, Spain (Current).*
**email: d.manzanal@upm.es*

ABSTRACT

The efficiency of calcium lignosulfonate (CLS) as an expansive soil stabiliser was studied. CLS is a bio-based polymer, obtained as a sub-product of the paper industry. Its use as a soil stabilizer not only enhances the properties of the soil but also eliminates the economic and environmental costs of its disposal. In this project, CLS was added to a natural smectite clay (Clay) from Comodoro Rivadavia, Argentina. Smectite clays exhibit significant plastic volumetric deformations when subjected to moisture variations. Clay was stabilised using 3.0 and 5.0% mass of CLS. The efficiency of CLS as a stabilising agent was measured studying its influence on the physical properties of Clay (Atterberg limits, Cation Exchange Capacity, Specific Surface Area). Considerable reductions of the cation exchange capacity (CEC) and the specific surface were registered. Furthermore, a full hydro-mechanical characterisation of Clay with CLS was performed in saturated and unsaturated conditions. Results from free swell and swelling pressure tests show that CLS reduces by nearly a half and nearly a quarter the free swell and swelling pressure of Clay, respectively. Additionally, mercury intrusion porosimetry (MIP) and scanning electron microscopy (SEM) tests were carried out to evaluate the microstructure re-arrangement of Clay when CLS was added. Results showed that a relatively small amount of CLS might yield a reasonably satisfactory performance as a stabiliser, particularly in reducing the natural Clay's swelling potential. Moreover, CLS induced an increase in the stiffness and strain at failure of Clay and a reduction in its porosity.

KEYWORDS: expansive clay, swelling soil, lignosulfonate, soil additive, microstructure, ground improvement.

1) INTRODUCTION

Expansive soils are responsible for volumetric changes that produce detrimental effects on civil engineering constructions. Lightweight structures, such as houses and pavements, are affected when founded over them (Bowles, 1978; Juárez Badillo & Rodríguez, 2000). Deep and slab foundations are some of the typical solutions projected to avoid these problems.

To reduce these detrimental effects of founding over expansive soils, a previous stabilisation treatment is generally performed. Stabilisation treatments are performed to enhance the properties of the natural soil at the project site until it reaches the desired properties. Several additives are used to achieve this goal as, for example, lime, cement, fly ash, and different pozzolanic additives (Croft JB, 1964; Hoyos et al., 2004; Pedarla et al., 2011; Goodarzi et al., 2016; Bicalho et al., 2018). These traditional stabilisers yielded a satisfactory performance over the last decades. Nevertheless, some of them tend to increase the pH of pore water over nine, meaning a possible problem to alkaline-sensible ecosystems (Vinod et al., 2010; Indraratna et al., 2010). In these cases, a more acidic stabiliser would be appropriate.

During the last decades, a great effort has been made to replace industrial synthetic materials to bio-based materials and even biodegradable materials, when their application allows it. Additionally, the reuse of by-products gained particular interest since it makes them valuable. Furthermore, the use of polymers in geotechnical engineering has found different applications, including soil stabilisation. Calcium lignosulfonate, also known as CLS, is a bio-based polymer, obtained as a by-product of the paper industry. Using this polymer as a stabiliser for expansive soils achieves a double objective of reducing the soil expansion and providing a use for this by-product, thus eliminating the economic and environmental cost of its deposition.

Lignosulfonates and oil lignosulfonates reduce the water adsorbed between layers making it easier to compact clayey soil (Camacho Tauta et al., 2006). Furthermore, Seco et al. (2011) reported that additives with cations such as Ca^{2+} and Mg^{2+} reduce the repulsive forces between clay layers inducing them to flocculate. This flocculation reduces soil plasticity, increases permeability, reduces its expansion and increases the bearing capacity.

Canakci et al. (2015) studied different additives, such as lignin, rice powder and rice ash as soil stabilisation agents. They reported a reduction of 50% of the plasticity index of the expansive soils with the addition of 15% mass of lignin, an increase in the unconfined compressive strength (UCS), and an overall increase in the strength of the natural soil for long curing periods.

Alazigha et al. (2016) studied the effect of different percentages of CLS on natural soils. The natural soil modified with 2.0% mass CLS reduced the free swell and swelling pressure by 20%. Furthermore, Alazigha (2017) compared the addition of 2% CLS treated soil with 2% cement-treated soil and the untreated soil. Both CLS and cement addition changed the expansibility classification from highly expansive soil to low expansive soil. UCS increased for both samples in comparison to the untreated soil, 7% higher for 2% CLS and 11% higher for the 2% cement. The sample with 2% CLS increased its ductile behaviour. During the consolidation test, both samples with cement and CLS behave no longer like clayey soils, but more like silts (bigger particle size or more aggregated particles) yielding primary consolidation in less time. Finally, the permeability calculated during the consolidation tests presented similar values for the untreated soil and the soil with 2% CLS, particularly at consolidation pressures over 100 kPa. This effect was attributed to a less connected pore flow, promoting the hypothesis of more aggregated particles (Alazigha et al., 2018).

This work studies the effectiveness of a bio-based by-product of the paper industry, CLS, as a stabilisation agent for a highly expansive clayey soil from Comodoro Rivadavia, Argentina (Clay). This clay of marin origin belongs to a geological formation called Patagonia which is composed exclusively of marine sediments of the Neritic type (oceanic deposition environment, up to a depth of approximately 180 meters) found in the surroundings of the city of Comodoro Rivadavia (Giacosa et al., 2004). This soil had repeatedly presented problems in lightweight constructions. Several researchers are studying the behaviour of this soil as part of an ongoing project that aims to control, avoid or reduce its expansiveness (Ruiz et al., 2012; Orlandi et al., 2015; Marti et al., 2015; Orlandi et al., 2016; Pique et al. 2019, Orlandi et al., 2019, Manzanal et al., 2019, Codevilla et al., 2019).

The efficiency of CLS as a stabilisation agent was evaluated experimentally. The physical and hydro-mechanical properties of both saturated and unsaturated Clay with CLS were measured, as well as the free swell and swelling pressure. Additionally, to understand the interaction between Clay and CLS, the porosity and the morphology were analysed.

2) MATERIALS

Clay

Natural smectite clay from San Jorge gulf basin, extracted from a surficial deposit of Comodoro Rivadavia, Argentina was studied (Clay). The clay has high plasticity with moisture content at the liquid limit (LL) of 80%, at the plastic limit (PL) of 39% and 25% at shrinkage limit (SL). Physical and chemical characteristics are presented in **Table 1**. It can be observed that Na^+ is a predominant cation, although Ca^{2+}, Mg^{2+} and K^+ are also present. The clay has a relatively low sulphate concentration (3608 ppm). The specific surface of Clay, measured using the maximum adsorption of methylene blue, according

to Santamarina et al. (1994), is higher than 563 m^2/g. According to the Unified Soil Classification System (USCS), Clay is classified as MH.

Calcium Lignosulfonate

Calcium lignosulfonate (CLS) is a brownish powder kindly provided by GCP S.R.L. Some physicochemical characteristics of the product, provided by the manufacturer, are listed in **Table 2**.

3) METHODS

X-ray diffraction analysis of Clay was conducted in a Philips 3020 diffractometer using radiation CuKα Ni filter (at 35 kV, 40 mA). Scanning is done between 3° and 70° 2θ, with a step of 0.04° and a count time of 2 s/step. The openings of the divergence, reception and dispersion slots are 1,0,2 and 1° respectively, and monochromator was not used. With an X'Pert High Score program, mineral phases were identified and quantify following Moore and Reynolds (1997) procedures.

Samples were studied using Infrared Spectroscopy (IR) to evaluate the compatibility between Clay and CLS. IR spectra of samples were analysed using KBr as a reference, recording the transmittance in the region 4000-600 cm^{-1} at a resolution of 4 cm^{-1} in a Shimadzu IRAffinity.

The pore size distributions of the compacted specimens were characterised through mercury intrusion porosimetry (MIP) according to ASTM 2873 in a Pascal 440 Thermo Fisher, for measuring pores size between 7 nm to 13 000 nm, and Pascal 140 Thermo Scientific, for measuring pores size between 13 000 nm to 100 000 nm. Samples were compacted statically at the desired water content in a mould, with a minimum volume of 1 cm^3. After compaction, samples were dehydrated by freeze-drying technique (Delage & Lefebvre, 1984). First, samples were frozen by immersion in liquid nitrogen. Then,

samples were placed directly in the freeze-drying equipment at 50ºC and 2 Pa for three days were they dried by sublimation (Laccomo model FreeZone 2.5 76705). This procedure minimises the influence of the drying process on the structure of the soil skeleton (Birle, 2012; Delage & Lefebvre, 1984).

The morphology of the samples was studied using scanning electron microscopy (SEM) within a Phenom-World ProX. For SEM images, small samples portions were mounted on aluminium stubs with carbon coating to ensure conductivity through the sample. Samples were conditioned as for MIP.

The Expansion Index (EI) tests were executed according to ASTM D4829 standards. The EI parameter is defined as 1000 times the specific vertical deformation of a sample free to swell during twenty-four hours. Samples were prepared using dry materials (Clay and CLS). Deionised water was added to achieve the desired moisture content and the sample was left for 24 hs to ensure the moisture homogenization prior compactation. The mould consisted of a three pieces cylinder of 101.6 mm diameter. The middle ring, in which the test was performed was 25 mm high. The sample was compacted dynamically with fifteen uniformly distributed blows of a rammer in free fall of 305 mm of height for each layer, in two layers of equal volume. Scarification was done to increase friction between each layer. Finally, the apparatus was dismantled, and the middle ring used to perform the test. The surplus soil was trimmed to fit the height of the ring, and a 6.9 kPa load was applied for at least 10 minutes before flooding the sample and starting the test. After ten minutes, the sample was ready, and then the ring was placed in a watertight container where a retractable anvil and an indicator for precise deformation measurements were placed over the sample to compute heave.

ASTM standard for this test allows the calculation of EI_{50} for samples with an initial degree of saturation between 40% and 60%. The EI between these degrees of saturation can be extrapolated to EI_{50}, corresponding to a degree of saturation of 50%.

The free swell was measured according to ASTM D4546 in an oedometer apparatus. The free swell test defines the expansiveness capacity of the soil, which can be expressed as the percentage of height variation. The test consists of flooding a sample of 18 mm height and 76 mm diameter with deionised water while measuring its height variation. This test is finished when the sample reaches an asymptotic behaviour of height variation in a log scale time graph.

Swelling pressure is the pressure applied to a sample that restricts it from swelling. In this work, the swelling pressure was considered equal to the pressure that reduced the height of an expanded sample to its initial height. The sample was statically compacted in one layer into a mould of approximately 18 mm height and a diameter of 76 mm. It was then mounted in an oedometer apparatus, flooded under a pressure load of approximately 5 kPa, and allowed to swell until an asymptotic behaviour in time log scale was reached. After the sample had expanded and reached its final height, loading steps were applied to determine the swelling pressure. For each loading step, its height variation was recorded until it reached an asymptotic variation in a time log scale, which is the end of the primary consolidation, and the corresponding void ratio was reported. Load increments were repeated until the void ratio of the specimen after swelling (e_s) reached the initial compaction void ratio (e_0). This pressure is the specimen's swelling pressure.

Unconfined compressive strength (UCS) was measured according to ASTM D2166 standard in a Controls-Wykeham Farrance Tritech 50 kN testing machine. Samples were compacted statically in three equal volume layers in a three-piece cylinder, 38 mm diameter and 76 mm height. Scarification was done to provide continuity between layers.

The specimen was compressed at a constant displacement rate determined as the 10% of the specimen height. Force (N) and displacement (mm) were automatically recorded during the test. The initial elastic and the secant modulus were determined.

For determining soil suction, the filter paper method test was used, according to ASTM D5298 and Bulut & Leong (2008). The procedure consists in measuring the moisture content of a calibrated filter paper in contact with soil (matric suction) or in equilibrium with the partial vapour pressure in a sealed container with no more than 1ºC temperature fluctuation (total suction). Samples require a minimum of seven days to reach a hygroscopic balance between the filter paper and the soil mixtures. A precision weighing balance is used to measure the moisture content of the filter paper. The ASTM standard proposes the calibration of the gravimetric water contents of the filter paper Whatman No. 42 and suction measured adopted for this study.

In order to obtain both, matric and total suction, two soil specimens of 100 mm diameter and 25 mm height were compacted. A set of three filter papers were placed between the samples to measure the matrix suction. The filter papers in contact with the sample had a larger diameter (100 mm), while the one in the middle a smaller one (90 mm). The smaller filter paper is subtracted quickly, and the increase of its weight registered. Muñoz-Castelblanco et al. (2012) presented a procedure in which they change the initial moisture of the filter papers to determine the hydraulic hysteresis of the material. In this series of tests, the filter papers were previously oven-dried. The total suction was measured, placing two extra sets of filter paper over the upper soil sample avoiding contact between the specimens. The sets were placed in a sealed container to gain a moisture equilibrium for seven days before measuring the moisture of the filter papers. Compacted samples were prepared to start from different water content with a targeted dry density.

There is a link between the water retention curve (WRC) and the pore size distribution (PSD) of a soil sample obtained with MIP since the interface between the non-wetting fluid (air in case of WRC or liquid Hg in case of MIP) and the wetting fluid (water and air, in case of WRC or Hg vapour for MIP) is governed mainly by capillarity. MIP can be related to the drying path of the initially saturated sample by applying an increase of external air pressure (non-wetting fluid) (Romero, 1999; Muñoz-Castelblanco et al., 2012).

Sample preparations: CLS – Clay admixture

Clay was firstly mixed with two different mass percentages of CLS to clay: 3% (Clay + 3% CLS) and 5% (Clay + 5% CLS). Physical (Atterberg Limits, Specific Surface) and chemical (FTIR, CEC) tests were performed on the mixtures.

The hydraulic and mechanic behaviour of compacted Clay and Clay + CLS was characterised. For Clay + CLS mixtures, 105ºC oven-dried Clay was mixed with CLS. The mixtures were wetted to the desired water content and stored in an airtight container for at least twenty-four hours to homogenise the moisture content. Finally, samples were statically compacted to the desired dry density.

Mixtures were submitted to a standard Proctor compaction method (ASTM D698) to select the initial densities and water contents for the tests. The maximum dry density (γ_{dmax}) and 95% of the maximum dry density ($\gamma_{d95\%}$) are reported in **Table 3**.

Clay and Clay + CLS mixtures were tested at the same dry density and moisture content. The targeted dry density was 12.4 kN/m^3, equal to the 95% of the maximum standard Proctor γ_d of Clay. The moisture content at dry of optimum (ω_{dry}), at optimum (ω_{opt}) and at wet of optimum (ω_{wet}) were also obtained from Standard Proctor curve of the Clay at the target dry density (**Table 3**).

4) RESULTS AND DISCUSSION

CLS – Clay interaction

Smectite (Sm) with impurities of calcium (Ca^{2+}) and feldspar (F) was identified within the XRD diffractogram of Clay, as is shown in **Figure 1**. The interaction between CLS and Clay was firstly analysed by considering how CLS affects basic geotechnical properties of Clay (**Table 4)**. Calcium-rich additives used to stabilise highly expansive clays, such as CLS, require the verification of sulphate concentration. It should be lower than 8000 ppm to avoid the formation of ettringite and thaumasite. These minerals can produce considerable expansion (Mitchell and Dermatas, 1992; Puppala et al.,2005). The soil studied presented lower sulphate concentration of 3608 ppm.

Clay was mixed with 3% (Clay + 3% CLS) and 5% (Clay + 5% CLS) in mass of CLS to dry mass of clay. The addition of CLS to Clay increased the Atterberg Limits, which may be interpreted as a contradiction to the positive effect of CLS treatment in terms of reducing Clay's swelling potential. Nevertheless, it decreased the specific surface (Se) and cation exchange capacity (CEC), both obtained by the method proposed by Santamarina (1994). These parameters are closely related to the expansiveness of clay, the smaller the Se and the CEC, the lesser the clay would expand with water. This contradiction may present an incompatibility when using these admixtures and try to classify them with traditional classification methods since most of them are based on plasticity index properties. Orlandi et al. (2019) analysed the variation of the Atterberg Limits of a highly expansive clay for different dosages of different types of lignins. They did not find a clear trend in the LL and IP when adding CLS.

Samples were initially studied using Infrared Spectroscopy to evaluate the compatibility of Clay with CLS (**Figure 2**). The main bands of Clay agree with those reported in different works (Venkatathri, 2006; Castro & Coral, 2013; Da Silva & Guerra, 2013).

These researchers reported that natural clays usually present a broad band between 3680-3160 cm^{-1} that corresponds to O-H stretching vibration of water coordinate to hydroxyl groups and Al, Si, and Mg ions. The peaks at Si-O stretching 1624 cm^{-1} would correspond to the presence of water in the silicate structure, and the band at 1120 cm^{-1} is due to siloxane stretching (Si-O-Si). Lastly, the band at 870 cm^{-1} and 800 cm^{-1} correspond to Si-O stretching and vibrations.

The main bands of CLS are also in agreement with those reported in previous works (Ortiz, 2009; Boeriu et al. 2004). These works report that lignosulfonate usually present a broad band 3600-3300 cm^{-1} that corresponds to hydroxyl groups in phenolic and carboxylic acids. The peak at 2940 cm^{-1} would correspond to a C-H stretching, and the band at 1770 cm^{-1} is due to aromatic acetoxy groups. In the region from 1900 to 800 cm^{-1}, known as the fingerprint region, several bands with variable intensity are observed. There is a shoulder at 1700 cm^{-1} which corresponds to aromatic acetoxy groups, bands at 1623 cm^{-1} which corresponds to unconjugated carbonyl carboxyl stretching, C=C vibrations bands at 1513 cm^{-1}, C-H deformations and aromatic ring vibrations at 1450 cm^{-1}, more C-H deformation at 1171 cm^{-1} and C-O and C-C vibrations associate with COH bending at 1050 cm^{-1}. Lastly, the band at 645 cm^{-1} was assigned by Ortiz (2009) to S-O stretching vibration of the sulfonic groups.

When testing Clay + 3% CLS and Clay + 5% CLS, bands of CLS were visible, especially in the range between 1600 cm^{-1} and 1000 cm^{-1} that correspond to deformation and vibrations of the aromatic groups of CLS. The same was found by Vinod et al. (2010) who took this result as a confirmation of a bonding formation between the clay minerals and lignosulfonate.

The microstructure of compacted CLS-Clay samples

Figures 3 and **4** show the pore size distribution curves of Clay and Clay + CLS. Graphs are presented in terms of both density functions and cumulative intruded void ratio where the intruded pore radius is represented on the logarithmic scale x-axis. The pore size density distribution presented in **Figure 3** shows two dominant pore size on the dry of optimum moisture content (ω_{opt}) for Clay and Clay + CLS as obtained by different authors (Romero, 2011; Alonso et al. 2013). These two dominant pore sizes are referred to as micro-porosity (7 to 80 nm approximately) and macro-porosity (7000 to 70000 nm). Regarding the micro-porosity, it is noted that the most frequent microstructural pore size of Clay is bigger than the most frequent microstructural pore size of both Clay + 3% CLS and Clay + 5% CLS. This can be related to a microstructural void ratio reduction with the CLS addition as it showed a significant reduction of both cation exchange capacity and specific surface for both studied samples. Indraratna et al. (2010) proposed a stabilisation mechanism in which CLS formed a chain that entered between clay particles, neutralising electric charges of the surface of the clay, holding the clay particles together. The neutralisation of electric charges in clay surface reduce the repulsive forces between clay particles. This effect can be related to the microporosity decrease.

Regarding the macro-porosity, the smallest pore characteristic size was obtained for Clay + 3% CLS mixture, followed by the untreated Clay and Clay + 5% CLS mixtures respectively. However, considering the void ratio, it is noted that CLS reduced the porosity in 5% for Clay + 3% CLS and 11% for Clay + 5% CLS as can be observed in **Figure 4**. The micro and macro-structural void ratio portions can be obtained according to Delage and Lefebvre (1984) throughout the intrusion and extrusion on MIP. These authors defined micro-porosity as the reversible portion of mercury extruded from the samples when the pressure of mercury is diminished (**Figure 4**). This is related to the

microstructural configuration of the sample, the surface charges of clay platelets and the non-wettability of mercury. The macro-porosity portion of the sample is the non-reversible mercury volume stacked in the sample. The macro void ratio is calculated as the initial void ratio minus the micro void ratio, which is the last registered void ratio of the test. The results showed that the macro void ratio decreased with the addition of CLS, e_M = 0.52 for Clay, e_M = 0.45 for Clay + 3% CLS and e_M = 0.44 for Clay + 5% CLS. The decrease in the pore volume due to CLS can be observed on SEM images of compacted samples with different percentages of CLS with moisture content at dry of optimum (ω_{dry}) (**Figure 5a**) and wet of optimum (ω_{wet}) (**Figure 5b**).

Expansion Index, Free swell, swelling pressure and consolidation analysis

The presence of smectite with predominately Na^+ cations explains the high swelling potential of Clay (Al-Rawas, A. A., 1999). Six samples were tested to obtain the average expansion index of each mixture. **Table** shows the results with an evaluation given by ASTM D4829. There is a reduction of the expansion potential for increasing percentages of CLS, according to the results obtained for specific surface and cation exchange capacity. When adding 3% of CLS, the potential expansion decreases from “high” to “medium”, and when adding 5% of CLS, it decreases “high” to “low”. These results constitute an engaging approach to expansiveness reduction considering these tests have a constant time length generally much smaller than free swell tests.

Free swell tests were conducted to confirm this proposition. These provide the total expansion of the soil mixtures. After reaching the total expansion, samples were subjected to loading steps. The initial conditions and the results of the tests are presented in **Figure 6**. The free swell of the untreated Clay was 32%. Clay with 3% and 5% of CLS presented a reduction of the free swelling of 40% and 45% respectively. This result confirms that

CLS reduces the swelling capacity of Clay (Alazigha et al., 2016; Alazigha et al., 2018). Alazigha et al. (2016) observed that the reduction in the expansiveness of a CLS treated sample is due to the binding of soil minerals due to CLS through basal and peripheral absorption. The CLS absorption restricts the infiltration of moisture into the soil and reduces the free swelling. The swelling reduction for higher CLS dosages does not present a linear trend.

The swelling pressure was determined as the pressure applied to the sample, after completing the free swell phase, that reduces the void ratio after swelling (e_s) to the initial void ratio before swelling (e_0) (**Figure 7**). The swelling pressure of the Clay also decreased with the addition of CLS from 845 kPa to 240 kPa for Clay + 3% CLS and 330 kPa for Clay + 5% CLS. The swelling pressure reduction was 70% for Clay + 3% CLS and 60% for Clay + 5% CLS.

The compressibility index (C_c) of the samples (**Figure 7)** was calculated as the ratio between the void ratio variation and the vertical stress variation on the virgin compression regime. Compressibility index (C_c) results show that the addition of CLS does not present a clear trend for the percentages studied. The compressibility of Clay + 3% CLS increased 27% in comparison with Clay, while for Clay + 5% CLS it was reduced by 33%. These opposite modifications on samples' compressibility and their similar free swell reduction are the reasons for finding a more significant reduction of the swelling pressure for the Clay + 3.0% CLS than Clay + 5.0% CLS. Therefore, considering the results for both free swell and swelling pressure for the Clay + CLS samples, it is possible to establish that both samples have similar swelling reduction potential but generate different mechanical properties variations over the Clay. As for engineering purposes, lesser compressible soils are convenient; therefore, the addition of 5% of CLS to Clay presents a more suitable modification.

During consolidation, the consolidation coefficient (C_v) and the permeability (k) were calculated. The results show a reduction of k and C_v for Clay with CLS addition. Therefore, the addition of CLS generated an admixture with lower porosity or less connected porous arrangement. Conventional one-dimensional consolidation tests were performed on specimens at full saturation with vertical stresses of 25, 112, 230 and 460 kPa. The first consolidation time was calculated using the square root of time, and the results can be found in **Table 6**.

The C_v of Clay and Clay + CLS decreased with increasing pressures. The general trend in **Figure 8** shows that Clay has the higher C_v and Clay + 3% CLS has the lowest for each seating pressure, only in the last step Clay + 5% CLS has the lowest C_v. The results for C_v varied from 3.1 10^{-8} m^2/s for Clay at 25 kPa to as low as 1.8 10^{-10} m^2/s for Clay + 5.0% CLS at 460 kPa.

C_v registered a rapid initial settlement for the initial loading steps and then, for higher pressures, remained almost constant. For Clay, the first three loading steps showed a rather substantial reduction of C_v with a lower C_v variation at the last loading step. Clay + 3.0% CLS showed a rapid initial settlement only in the first loading step, with an approximately constant C_v for the following steps. For Clay + 5.0% CLS, the behaviour showed almost a linear trend for all tested the loading steps. The obtained results for the Clay + 3% CLS sample for different loading pressures implies that after the initial short-term settlement, the settlement for increasing pressures will remain approximately constant. The registered behaviour for Clay + 3% CLS does not represent typical clayey soil under increasing pressures, as it tends to an asymptotic settlement for increasing pressures. This behaviour was not found in the tested loading steps for Clay + 5% CLS.

Figure 8 shows that Clay + CLS has a permeability coefficient in the range of half of the Clay, which may be related with a less connected porous arrangement. The permeability

varied from 3.3 10^{-10} m/s for Clay at 25 kPa to 3.2 10^{-13} m/s for Clay + 5% CLS at 460 kPa. As expected, the variation of k of the three samples presented very similar trends than those obtained for C_v. Permeability had a significant decrease for the first loading step and then became approximately constant for Clay + 3% CLS, the permeability of Clay + 5% CLS decreased linearly. This finding shows that CLS produced a slight reduction in permeability due to the decrease of macro-porosity observed in MIP. Similar results were observed by Alazigha et al. (2018).

Unconfined Compressive Strength

Unconfined compressive strength (UCS) was measured to characterise the unsaturated compressive strength of the different mixtures at the different initial moisture content (dry of optimum, optimum and wet of optimum). The stress-strain graphs of all the samples are plotted in **Figure 9**. Additionally, two lime treated samples (Clay + 3% Lime and Clay + 5% Lime) were included in at wet of optimum moisture content.

Results show an increase of the UCS for Clay + 5% CLS for the three compaction moisture contents. This increase when compaction moisture content was set at the dry of the optimum was 47%, at optimum 5% and at wet of the optimum 25%. In the case of Clay + 3% CLS, only when the initial moisture content was set at the dry of optimum, the UCS increased by approximately 21%. Clay + 3% CLS with the optimum and wet of optimum moisture content presented a decrease of UCS of 8% and 1%. These results suggest that Clay + 3.0% CLS does not improve the mechanical properties of the clay as expected, even though the decrease of the UCS is lower than 10%.

Clay with CLS presented a more ductile behaviour, reaching the maximum compressive strength with lager axial strain. Both Clay + CLS samples compacted at dry of optimum moisture content registered an increase in the deformation at the failure of about 50%.

For optimum moisture content, the deformation at failure was equal to that of untreated Clay when CLS was added at 3.0% and increased by 50% when it was added at 5.0%. Finally, for samples compacted at wet of optimum moisture content, it increased 75% and 150% for Clay + 3% CLS and Clay + 5% CLS respectively. However, comparing the UCS between the three moisture contents (wet, optimum and dry) for equal CLS content, a decrease in uniaxial strength is observed for the samples on the wet of optimum moisture content. Clay + CLS have smaller secant stiffness than Clay in all the cases but for Clay + 5% CLS with an initial moisture content set at the dry of optimum. S

Considering the results obtained from the Clay + 3% Lime and Clay + 5% in **Figure 9c** there is an expected difference in the UCS values. The increments of the resistance vary from six to seven times bigger. Considering the deformation at failure, these samples registered a deformation similar to the one obtained with the untreated clay and from 15% to 40% smaller than CLS treated samples. Differently from CLS treated samples the secant and initial stiffness modulus for both lime treated samples are similar to each other with variations in the order of 15% maximum.

The smaller stiffness was expected since the increase of the strength at failure is not the same as the increase of the strain at failure, and for most of the Clay + CLS samples, the ratio between strength and strain was smaller. The secant stiffness modulus, which is related to the strength and strain at failure, decreased 18% at dry of optimum moisture content, 9% at optimum moisture content and 44% at wet of optimum for Clay + 3.0% CLS. The secant modulus of Clay + 3.0% C increased 9% at dry of optimum moisture content but decreased 47% and 49% at optimum and wet of optimum moisture content respectively. Although there is an overall increase in the unconfined compressive strength for Clay + CLS, the stiffness is generally smaller.

Soil-Water Retention Curve

The water retention capacity of the unsaturated compacted samples of Clay and Clay + CLS were obtained using the filter paper method (ASTM D5298). This technique allows estimating the relationship between the degree of saturation and suction at equilibrium for compacted samples at a given density and different initial water content of Clay, Clay + 3% CLS and Clay + 5% CLS. Experimental results are presented in **Figure 10** in terms of suction and degree of saturation. The samples had an average dry density of 12.4 kN/m^3 (e = 1.130 - 1.250), except for Clay + 3% CLS - UNPSJB samples with slightly higher average densities (e = 0.750 - 0.940). Clay + CLS presented fairly scattered results for the same dry density. For a certain degree of saturation, it is observed that the estimated suctions of Clay with 3.0% and 5.0% of CLS are larger than Clay. However, the estimated suction increment with the increase in the CLS dosage is rather small.

Results were modelled with the van Genuchten equation (van Genuchten, 1980). Equation (1) describes the soil-water retention curve. This equation relates the matric suction $(u_a - u_w)$ and the degree of saturation of the sample (S_r). The effective degree of saturation (S_e) varies from 0 to 1. It equals unity when samples are saturated, even for matric suctions bigger than 1. The value of suction in which desaturation begins is called air-entry value suction (S_{ae}). S_e equals zero when the residual degree of saturation (S_{res}) is reached. S_{res} is the approximately constant value of the degree of saturation regardless of the increasing matric suction. This residual water content is trapped in the microstructure of the soil. Therefore, residual degree of saturation or residual water content is related to the microporosity of the sample obtained within mercury intrusion porosimetry (MIP) (Romero, 1999). Finally, λ is a fitting parameter that considers the pore size distribution of the soils. For more aggregated or coarse-grained soils, λ is expected to be higher.

$$S_e = \frac{S_r - S_{res}}{S_{sat} - S_{res}} = \left\{1 + \left[\frac{u_a - u_w}{S_{ae}}\right]^{1/1-\lambda}\right\}^{-\lambda} \quad (1)$$

The water retention curves fitted with the experimental data and the van Genuchten parameters are shown in **Figure10**. The results of the calibration suggest that CLS change the air entry value (S_{ae}) from 300 kPa to 600 kPa when 5% of CLS is added to Clay. This value is related to the suction that air must exceed to enter the pores of the soil, leading to the beginning of desaturation. MIP results showed that the addition of 5% of CLS to Clay reduced the frequency of large pores with an overall reduction of macro void ratio, which is consistent with the increment of the air-entry value (S_{ae}) of Clay + 5% CLS.

There is a slight decrease of λ (van Genuchten pore distribution parameter) with the addition of CLS, which agrees with the reduction in porosity observed in MIP performed on samples with an initial degree of saturation of 45%.

Romero (1999) related the residual water content (or the residual degree of saturation) to the difference between the void ratio measured through the intrusion of mercury during MIP test and the overall soil void ratio obtained from the compaction characteristics (dry density and water content). This difference would be the non-intruded void ratio Δe_{ni}. The residual water content is $100 \cdot \Delta e_{ni}/G_s$.

Figure 11 shows MIP results as a function of water content and suction together with the discrete results obtained by the filter paper technique. The residual water content obtained with MIP for the three samples analysed (Clay, Clay + 3% CLS, Clay + 5% CLS) varies from 20.0% to 21.3%. It is observed that the residual water content is not affected by the addition of CLS. The degree of residual saturation associated with these water contents and their respective void ratios vary between 44% and 48%. These results appear to be high, assuming that soils that contain a significant fraction of smectite cannot be fully intruded by mercury at 200 MPa (Lloret et al., 2003, Castelblanco et al., 2012). This

circumstance is directly related to the fact that the evolution of the void ratio curve maintains a slope in the area of the smallest pores (**Figure 4**). Therefore, there is a difference between the intruded void ratio and the overall soil void ratio. In this case, the smallest value reached with the MIP at 200 MPa is 7.4 nm (74 Å). Since the basic constituent of Clay is the elementary clay layer (9.6 Å thick for smectite), it can be implied that there might be several pores that were not intruded by the mercury (Delage et al., 2006).

In literature, there is some controversy when considering the residual saturation degree as a physical parameter (e.g. Luckner et al., 1989) or a calibration parameter (e.g. Fredlund & Xing 1994, Manzanal et al., 2010, 2011). In this work, the value was adopted according to the results obtained with MIP studying the work of Romero (1999) and using the calibration of the experimental results obtained by the filter paper method. **Figure 10** shows the experimental results with the van Genutchen model with the residual saturation degree for all samples equal to 30%. The samples used for the calibration of the van Genuchten model had a void ratio varying from e = 1.130 - 1.250

CONCLUSIONS

The present work studied the efficiency of calcium lignosulfonate (CLS) as a stabiliser of highly expansive clay. The interaction of clayey soil and CLS was examined by a series of tests for characterising the physical, hydraulic and mechanical properties of the three mixtures: a natural clay (Clay), the natural clay with 3% and 5% of CLS. Results showed significant changes in the physical and engineering properties. The following conclusions can be highlighted:

- The addition of CLS increased the liquid and the shrinkage limits of Clay, approximately 50% and 24%, respectively. The variation on the plastic limit was

less significant (8%). The results are similar for the two percentages of CLS studied. Atterberg Limits increment may be interpreted as a contradiction to the positive effect of CLS in terms of reducing the swell potential of the Clay. This contradiction may present an incompatibility when using these admixtures and trying to classify them with traditional classification methods. However, when the specific surface (Se) and cation exchange capacity (CEC) of untreated and CLS-treated samples were analysed, a substantial reduction of Se and CEC was observed with the increasing CLS percentages. These can be explained by the bonding formation between the clay minerals and lignosulfonate obtained by FTIR.

- The high Expansion Potential (EP) for Clay is reduced to "medium" for Clay + 3.0% CLS and to "low" for Clay + 5.0% CLS. The swelling capacity of Clay was reduced as well. This was demonstrated with the decrease of the free swelling of Clay with the addition of 3.0% and 5.0% of CLS, from 32.0% to 19.6% and 17.8%, respectively. In addition, the swelling pressure was reduced by 70% for Clay + 3.0% CLS and by 60% for Clay + 5.0% CLS. The compressibility of Clay + 3.0% CLS increased by about 30%, while the opposite occurred for Clay + 5.0% CLS, which decreased by about 30%. Hydraulic conductivity and the coefficient of consolidation of Clay decreased with the addition of CLS. Therefore, the addition of CLS generated an admixture with lower porosity or with a less connected porous arrangement. These results have been confirmed by mercury intrusion porosimetry, that registered a reduction of intruded void ratio with the addition of CLS. For the dry of optimum moisture content, CLS improved the UCS of the Clay. Only for Clay + 5.0% CLS this improvement was reported within the three tested moisture contents. For the samples compacted at the wet

of optimum and optimum moisture content, the increment of UCS was less significant. Clay + 3.0% CLS presented a lower UCS than the untreated clay. In terms of ductility, Clay + CLS reached the failure at higher deformations, increasing it up 150% for the wet of optimum moisture content in Clay + 5.0% CLS. Additionally, the stiffness of these samples dropped up to 50% due to the non-linear increase of strength-strain ratio.

- The addition of CLS increased the estimated suction for a given degree of saturation. However, the increment of suction with CLS dosage increase is rather small. Results suggested that the addition of 5% of CLS changes the air entry value (S_{ae}) of the van Genuchten model from 300 kPa to 600 kPa. This increment, which is consistent with the MIP results, showed that the addition of 5% of CLS reduced the frequency of large pores with an overall reduction of macro void ratio. The parameter λ from the van Genuchten model slightly decreased with the addition of CLS due to the reduction of the pore size distribution is reduced, as the MIP results showed. The CLS addition does not influence the residual degree of saturation evaluated within MIP.

Results showed that CLS yield acceptable performance as a soil stabiliser, particularly in reducing the natural Clay's swell potential even with no curing time. Further research is required to ensure its effectiveness on long-term behaviour, particularly after cyclic wetting-drying and cyclic freeze-thaw and the impact on longer curing times in experimental results. Moreover, the environmental impact (leachability) should be tested. Finally, constructability and cost-efficiency comparison is encouraged between CLS and traditional additives, bearing in mind the environmental costs of each additive.

ACKNOWLEDGMENTS

The authors acknowledge *Consejo Nacional de Investigaciones Científicas y Técnicas* (CONICET) and to the Agency of Scientific and Technological Promotion (*Agencia Nacional de Promoción Científica y Tecnológica*) from Ministry of Science and Technology of Argentine Republic. The authors also acknowledged the financials support of *Universidad Nacional de la Patagonia San Juan Bosco* (Project UNPSJBSYT PI1364) and *Secretaría de Políticas Universitarias* (MEYD-SPU) (Project "*Agregando Valor 2017 – Fundaciones Sustentables*" RESOL-2017-5157-APN-SECPU#ME). To the students Gaston Fernandez, Ignacio Cueto, Santiago Pastine, Nicolas Tasso and Camilo Casagrande, who collaborated with experimental work as part of their master theses.

REFERENCES

Alazigha, D.P., Indraratna, B., Vinod, J.S., Ezeajugh, L.E. (2016). The swelling behaviour of lignosulfonate-treated expansive soil. Proceedings of the ICE - Ground Improvement, 169, pp. 182–193.

Alazigha, D.P. (2017). Mechanisms of stabilisation of expansive soil with lignosulfonate admixture. Transportation Geotechnics, 14, 81-92.

Alazigha D.P., Vinod, J.S., Indraratna, B., Heitor, A. (2018). Potential Use of Lignosulfonate for Expansive Soil Stabilisation. Environmental Geotechnics. DOI: 10.1680/jenge.17.00051

Alonso, E., Pinyol, N., Gens, A. (2013). Compacted soil behaviour: initial state, structure and constitutive modelling. Geotechnique. 63(6), 463–478. DOI:10.1680/geot.11.P.134

Al-Rawas, A.A. (1999). The factors controlling the expansive nature of the soils and rocks of northern Oman. Engineering Geology, 533-4, 327-350.

Azzam, W.R. (2014). Durability of Expansive Soil Using Advanced Nanocomposite Stabilization. International Journal of GEOMATE, 7, 927–937.

Bicalho, K.V., Boussafir, Y., Cui, Y.J. (2018) Performance of an instrumented embankment constructed with lime-treated silty clay during four-years in the Northeast of France. *Transportation Geotechnics*, Volume 17, Part B, 2018, Pages 100-116, ISSN 2214-3912, DOI: 10.1016/j.trgeo.2018.09.009.

Birle, E. (2012). Effect of Initial Water Content and Dry Density on the Pore Structure and the Soil-Water Retention Curve of Compacted Clay. In C. Mancuso, C. Jommi, F. D'Onza, Unsaturated Soils: Research and Applications: Volume 1, 145-152. Berlin, Heidelberg: Springer Berlin Heidelberg.

Biscayne, P.E. (1965). Mineralogy and sedimentation of Recent deep-sea clay in the Atlantic Ocean and adjacent seas and oceans. Geol. Soc. Am., Bull. 76, 803-831. DOI: 10.1130/0016-7606

Boeriu, C.G., Bravo, D., Gosselink, R.J., van Dam, J.E. (2004). Characterisation of structure-dependent functional properties of lignin with infrared spectroscopy. Industrial Crops and Products, 20(2), 205-218.

Bowles, J. E. (1978). Engineering properties of soils and their measurement, 2nd ed. New York: McGraw-Hill.

Bulut, R., Leong, C. (2008). Indirect measurement of soil suction. Geotech. Geol. Eng. 26:633–644. Springer Science+Business Media B.V.

Camacho Tauta, J. F., Reyes Ortiz, O. J., Mayorga Antolínez, C., Méndez G., D. F. (2006). Evaluación de aditivos usados en el tratamiento de arcillas expansivas. Ciencia E Ingeniería NeoGranadina, 16(2), 45–53.

Canakci, H., Aziz, A., Celik, F. (2015). Soil stabilisation of clay with lignin, rice husk powder and ash. Geomechanics and Engineering, 8(1), 67–79. DOI: 10.12989/gae.2015.8.1.067

Castro, D. P., Coral, K. M. (2013). Caracterización y activación química de arcilla tipo Bentonita para su evaluación en la efectividad de remoción de fenoles presentes en aguas residuales. Universidad Tecnológica de Pereira, Escuela de Química, Química Industrial. Pereira, Riraralda.

Chen, R., Drnevich, V. P., Daita, R. K. (2009). Short-term electrical conductivity and strength development of lime kiln dust modified soils. *Journal of Geotechnical and Geoenvironmental Engineering*, 135(4), 590–594. DOI: 10.1061/(ASCE)1090-0241(2009)135:4(590).

Codevila, M, Casagrande, C., Fernandez, M., Piqué, T., Manzanal, D. Polymer enhanced clay-sand mixture. XVI Pan-American Conference on Soil Mechanics and Geotechnical Engineering 17-20 November 2019. Cancun, México

Croft, J. B. (1967) The influence of soil mineralogical composition on cement stabilisation. *Geotechnique* 17(2):119–135

Da Silva, R., Guerra, D. (2013). Use Of Natural And Modified Kaolinite/Ilite As Adsorbent For Removal Methylene Blue Dye From Aqueous Solution. Journal of Chilean Chemestry Society, 15(1).

Delage, P., Lefebvre, G. (1984). Study of the Structure of a sensitive Champlain clay and of its evolution during consolidation. Canadian Geotechnical Journal.

Delage, P., Marcial, D., Cui, Y. J. & Ruiz, X. (2006). Ageing effects in a compacted bentonite: a microstructure approach. *Geotechnique* 56, No. 5, 291–304, DOI: 10.1680/geot.2006.56. 5.291

Fredlund, D.G. and Xing, A. (1994) Equations for the Soil-Water Characteristic Curve. Canadian Geotechnical Journal, 31, 521-532.

Giacosa, R.E., Paredes J.M., Nillni, A.M., Ledesma M., Colombo, F..(2004) Fallas normales de alto ángulo en el Neógeno del margen Atlántico de la Cuenca del Golfo San Jorje(Spanish). Boletín Geológico y Minero, 115 (3): 537-550. ISSN: 0366-0176

Goodarzi, A. R., Akbari, H. R., & Salimi, M. (2016). Enhanced stabilisation of highly expansive clays by mixing cement and silica fume. Applied Clay Science, 132–133, 675–684.

Hoyos, L. R., Puppala, A. J., Chainuwat P. (2004). Dynamic properties of chemically stabilised sulfate rich clay Journal of Geotechnical and Geoenvironmental Engineering. 130: 153-162. DOI: 10.1061/(ASCE)1090-0241(2004)130:2(153)

Juárez Badillo, A., Rico Rodríguez, A. (2000). Soil mechanics. Mexico: Limusa.

Lloret, A. et al. (2003) 'Mechanical behaviour of heavily compacted bentonite under high suction changes', *Geotechnique*, 53(1), pp. 27–40. DOI: 10.1680/geot.2003.53.1.27.

Luckner, L., Van Genuchten, M. T., and Nielsen, D. R. (1989), A consistent set of parametric models for the two-phase flow of immiscible fluids in the subsurface, *Water Resour. Res*., 25(10), 2187–2193, DOI:10.1029/WR025i010p02187.

Manzanal, D., Pastor, M., Fernandez Merodo, M., Mira, P., 2010. A state parameter based Generalized Plasticity model for unsaturated soils. Computer Modelling in Engineering and Science CMES, vol.55, no.3, pp.293-317, 2010. DOI: 10.3970/cmes.2010.055.293

Manzanal, D., Pastor, M., Fernandez Merodo, M., 2011. Generalized plasticity state parameter-based model for saturated and unsaturated soils Part II: unsaturated soil modeling. Int. J. Numer. Anal. Met. 35 (18), 1899–1917. DOI: 10.1002/nag.983

Manzanal, D., Orlandi, S., Barria, J. C. (2019). Swell characterisation of expansive clays from Comodoro Rivadavia - Argentine. XVI Pan-American Conference on Soil Mechanics and Geotechnical Engineering 17-20 November 2019. Cancun, México. DOI:10.3233/STAL190107

Marti, L., Codevilla, M., Piqué, T. M., Manzanal, D. (2015). Natural soil modified with polymer for use in landfill system. Buenos Aires, Argentina: IOS Press. DOI:

10.3233/978-1-61499-603-3-2228.

Mitchell, J.K., Dermatas, D., 1992. Clay soil heave caused by lime-sulfate reactions. In innovations and uses for lime. ASTM STP 1135. *American Society for Testing and Materials*, Philadelphia, Pa., pp. 41–64

Moore, D.M., Reynolds, R.C. (1997). X-ray diffraction and identification and analysis of clay minerals. 2nd Edition, Oxford University Press, New York, United States of America.

Muñoz-Castelblanco, J.A., Pereira, J.M., Delage, P, Cui, Y. (2012) 'The water retention properties of a natural unsaturated loess from northern France', *Geotechnique*, 62(2), pp. 95–106. DOI: 10.1680/geot.9.P.084.

Orlandi, S., Manzanal, D., Espelet, A., Ruiz, A. (2016). About the use of soils as backfilling under roofs and flats: two study pathogy cases. Revista de Geología Aplicada a la Ingeniería y al Ambiente, 35, 103-114.

Orlandi, S., Manzanal, D., Miranda, E., Robison, M. (2019) Using lignin as stabiliser of swelling soils. XVI Pan-American Conference on Soil Mechanics and Geotechnical Engineering 17-20 November 2019. Cancun, México. DOI: 10.3233/STAL190295

Orlandi, S., Manzanal, D., Ruiz, A., Avila, M., Graf, M. (2015). A case study on expansive clays on Comodoro Rivadavia city. *In I. Press (Ed.), Proceedings of the 15th PCSMGE. 15-17 November*, 2276-2283. Buenos Aires, Argentina. DOI: 10.3233/978-1-61499-603-3-2276.

Ortiz, D. M. (2009). Lignosulfonatos de Zn adheridos en NPK como fertilizantes en cultivos de trigo y maiz. *Universidad Autónoma de Madrid*.

Pedarla, A., Chittoori, S., Puppala, A. (2011) Influence of mineralogy and plasticity index on the stabilisation effectiveness of expansive clays. *Transp Res Rec J Transp Res Board* 2212:91–99

Piqué, T., Manzanal, D., Codevilla, M., Orlandi, S. (2019). Polymer Enhanced Soils Mixture for Potential Use as Covers or Liners in Landfill Systems Environmental Geotechnics. Published Online: August 23, 2019. DOI: 10.1680/jenge.18.00174

Puppala, A., Intharasombat, N., Vempati, R., 2005. Experimental studies on ettringite-induced heaving in soils. *J. Geotech. Geoenviron*. 131 (3), 325–337

Rollings, R.S., Burkes, M.P. (1999). Sulfate Attack on Cement-Stabilised Sand, Journal of Geotechnical and Geoevnironmental Engineering, ASCE,125(5): 364-372.

Romero, E. (1999). Characterisation and thermo-hydro-mechanical behaviour of unsaturated Boom clay: an experimental study. PhD thesis, Universitat Politecnica de Catalunya, Barcelona

Romero, G. D. Della Vecchia, G. Jommi (2011). An insight into the water retention properties of compacted clayey soils. *Geotechnique*, 61 (4), 313–328. DOI:10.1680/geot.2011.61.4.313

Ruiz, A., Vargas, R., Manzanal, D. (2012). Estudio preliminar de las arcillas activas de la ciudad de Comodoro Rivadavia. *National Conference: Congreso Argentino de Mecánica de Suelos e Ingeniería Geotécnica - CAMSIG 2012*. Rosario, Argentina.

Santamarina, J. C. (1994). Soil Clasification: Physics foundation actual practice and recommedations. *Georgia, United States of America: 1st ed., Georgia Institute of Technology*, p. 1-6.

Sariosseiri, F., Muhunthan, B. (2009). Effect of cement treatment on geotechnical properties of some Washington State soils. *Engineering Geology*, 104(1–2), 119–125. https://doi.org/10.1016/j.enggeo.2008.09.003

Seco, A., Ramírez, F., Miqueleiz, L., García, B. (2011). Stabilization of expansive soils for use in construction. *Applied Clay Science*, 51(3), 348-352.

van Genuchten, M. T. (1980). A Closed-form Equation for Predicting the Hydraulic Conductivity of Unsaturated Soils. *Soil Science of America Journal*, 44: 892-898.

Venkatathri, N. (2006). Characterisation and catalytic properties of a naturally occurring clay, Bentonite. *Bulletin of the catalysis society of India*, 5, 61-72.

Vinod, J. S., Indraratna, B., Mahamud, M. A. A. (2010). Stabilisation of an erodible soil using a chemical admixture. *Institution of Civil Engineers. Proceedings. Ground Improvement*, 163 (1), 43-52.

LIST OF TABLES

LIST OF FIGURES

Figure 11: Comparison of gravimetric water content and degree of saturation using the filter paper technique with MIP results for the three mixtures: Clay, Clay + 3% CLS and Clay + 5% CLS.

TABLES

Table 1: Chemical and Physical properties of Clay.

	Test	Unit	Clay
Chemical compositions	SiO_2	[%]	58.7
	Al_2O_3	[%]	16.5
	Na_2O	[%]	3.8
	CaO	[%]	2.4
	Fe_2O_3	[%]	6.0
	MgO	[%]	2.4
	K_2O	[%]	1.4
	LOI	[%]	5.5
	SO^-_4	[ppm]	3608
	pH	[-]	8.51
Exchangeable Cation	CEC	[meq/100g]	74.4
	Na	[meq/100g]	28.5
	K	[meq/100g]	7.8
	Ca	[meq/100g]	16.2
	Mg	[meq/100g]	1.5

	Test	Unit	Clay
Physical properties	LL	[%]	80
	PL	[%]	39
	PI	[%]	41
	SL	[%]	24.7
	Gs	[-]	2.70
	$\gamma_{d\ max}$	[kN/m^3]	13.0
	ω_{opt}	[%]	31.0
	Se	[m2/g]	563
	#200	[%]	96.0
	Sand	[%]	4.0
	Silt	[%]	17.0
	Clay	[%]	79.0

Table 2: Technical report. CLS composition.

Analysis description	Unity	Technical specification	Typical values
pH (10% solution)	[%]	3.0-4.5	3.8
Moisture (at 105°C)	[%]	Max. 8.0	6.0
Ashes (at 800°C)	[%]	Max. 10.0	7.7
Calcium (as Ca)	[%]	1.5 – 2.4	1.8
Magnesium (as Mg)	[%]	1.4 – 2.2	1.8
Iron (as Fe)	[%]	Max. 0.1	0.04
Sulphur (as S)	[%]	Max. 8.0	6.0
Reductive substances		Max. 25.0	22.0
Colour	-	Brown	Brown
Water-insoluble	[%]	Max. 0.20	0.15
Density	[g/cm^3]	0.37 – 0.41	0.40

Table 3: Proctor Standard results.

			Clay	Clay + 3% CLS	Clay + 5% CLS
Compaction properties	γ_{dmax}	[kN/m^3]	13.0	12.4	12.5
	$\gamma_{d95\%}$	[kN/m^3]	12.4	11.8	11.9
	ω_{dry}	[%]	18.0	28.0	27.0
	ω_{opt}	[%]	31.0	34.0	35.0
	ω_{wet}	[%]	37.0	40.0	44.0

Table 4: Atterberg Limits, Specific Surface and Cationic Exchange results.

			Clay	Clay + 3% CLS	Clay + 5% CLS
Physical properties	LL	[%]	80.0	122.0	123.0
	PL	[%]	39.0	42.0	41.0
	SL	[%]	24.2	16.1	18.4
	Se	[m^2/g]	306.0	73.0	31.0
	CEC	[m_{eq}/100g]	77.4	65.1	7.8

Table 5: Expansion Index results.

			Clay	Clay + 3% CLS	Clay + 5% CLS
Expansion Index	Sr	[%]	43	46	44
	EI	[-]	114	71	40
	Potential expansion ASTM D4829	[-]	High	Medium	Low

Table 6: Permeability and coefficient of consolidation for each mixture[1].

		Clay		Clay + 3% CLS		Clay + 5% CLS	
	σ'_v	Cv	k	Cv	k	Cv	k
	[kPa]	[m^2/s]	[m/s]	[m^2/s]	[m/s]	[m^2/s]	[m/s]
Consolidation characteristics	25	$3.1\ 10^{-8}$	$3.3\ 10^{-10}$	$7.8\ 10^{-9}$	$1.0\ 10^{-10}$	$1.4\ 10^{-8}$	$1.3\ 10^{-10}$
	112	$1.1\ 10^{-8}$	$1.2\ 10^{-10}$	$2.2\ 10^{-9}$	$1.9\ 10^{-11}$	$5.0\ 10^{-9}$	$4.4\ 10^{-11}$
	230	$4.3\ 10^{-9}$	$2.8\ 10^{-11}$	$1.5\ 10^{-9}$	$1.1\ 10^{-11}$	$1.7\ 10^{-9}$	$9.9\ 10^{-12}$
	460	$3.9\ 10^{-9}$	$1.3\ 10^{-11}$	$2.2\ 10^{-9}$	$9.4\ 10^{-12}$	$1.8\ 10^{-10}$	$3.2\ 10^{-13}$

[1] Compaction characteristics in Figure 6 and Figure 7.

FIGURES

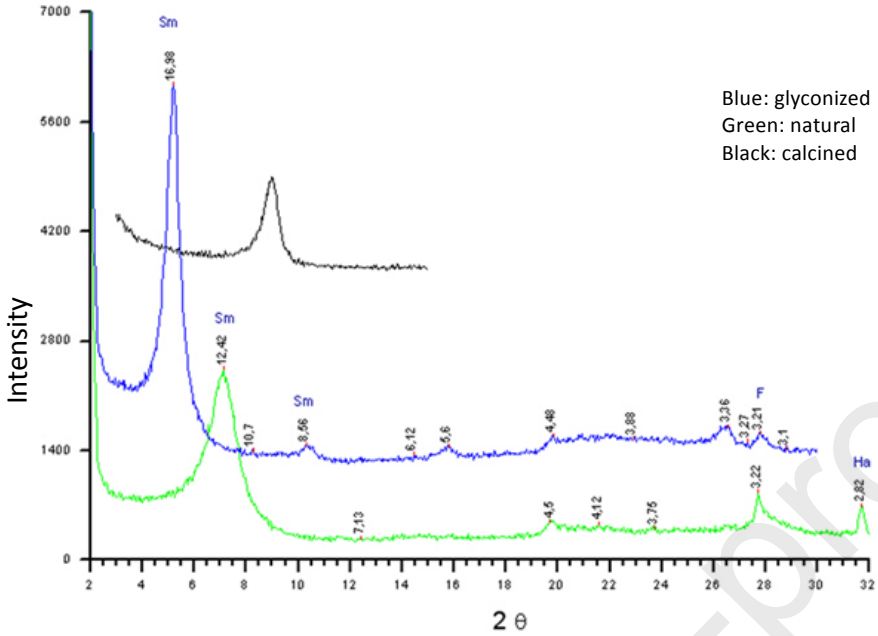

Figure 1: X-Ray Diffraction Clay by three methods: glyconized, natural and calcined.

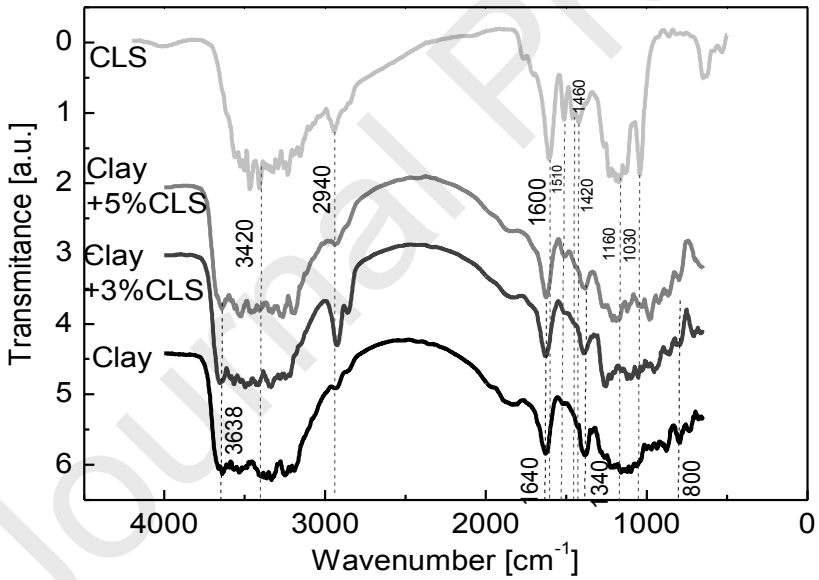

Figure 2: Infrared spectrum of CLS, Clay and Clay + 3% CLS and Clay + 5% CLS.

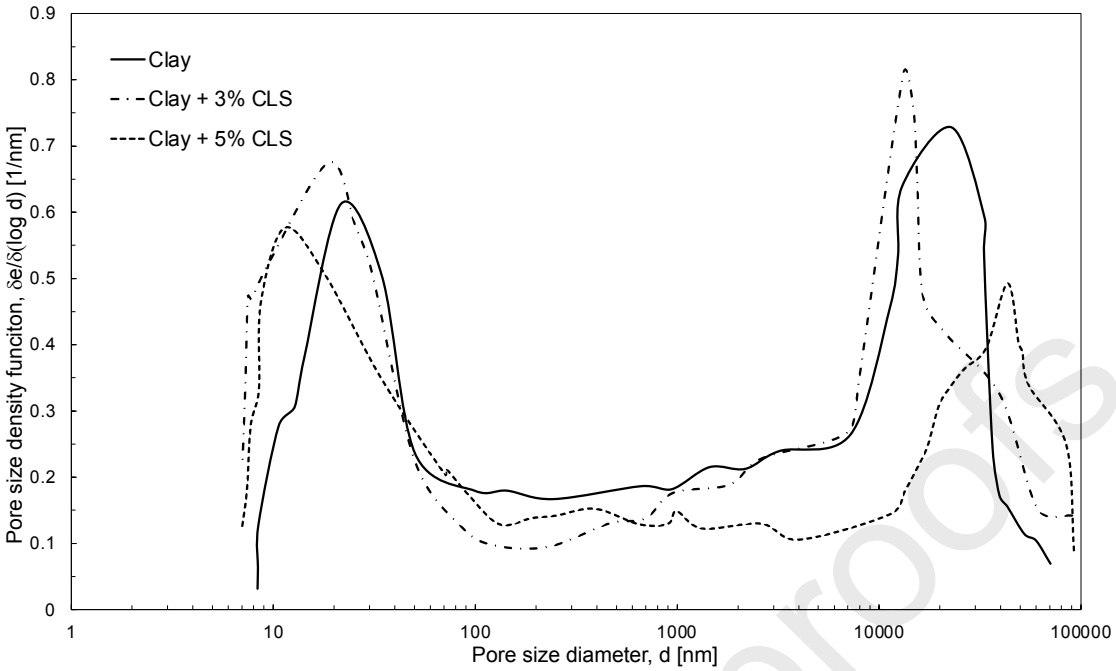

Figure 3: Pore size density distribution for the three mixtures obtained by MIP for Clay, Clay + 3% CLS and Clay + 5% CLS compacted samples at dry of optimum water content (Sr = 41% - 46%) and a given dry density (e = 1.18-1.23).

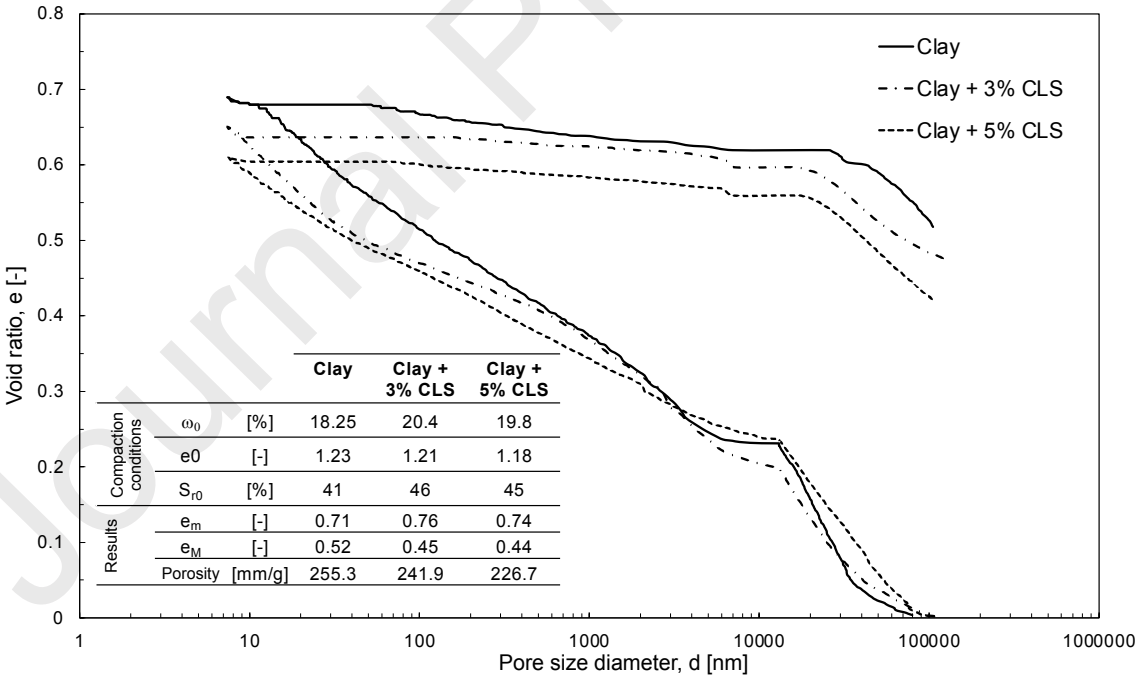

			Clay	Clay + 3% CLS	Clay + 5% CLS
Compaction conditions	ω_0	[%]	18.25	20.4	19.8
	e0	[-]	1.23	1.21	1.18
	S_{r0}	[%]	41	46	45
Results	e_m	[-]	0.71	0.76	0.74
	e_M	[-]	0.52	0.45	0.44
	Porosity	[mm/g]	255.3	241.9	226.7

Figure 4: Evolution of intruded void ratio obtained by MIP for the three mixtures: Clay, Clay + 3% CLS and Clay + 5% CLS compacted samples at dry of optimum water content (Sr = 41% - 46%) and a given dry density (e = 1.18-1.23).

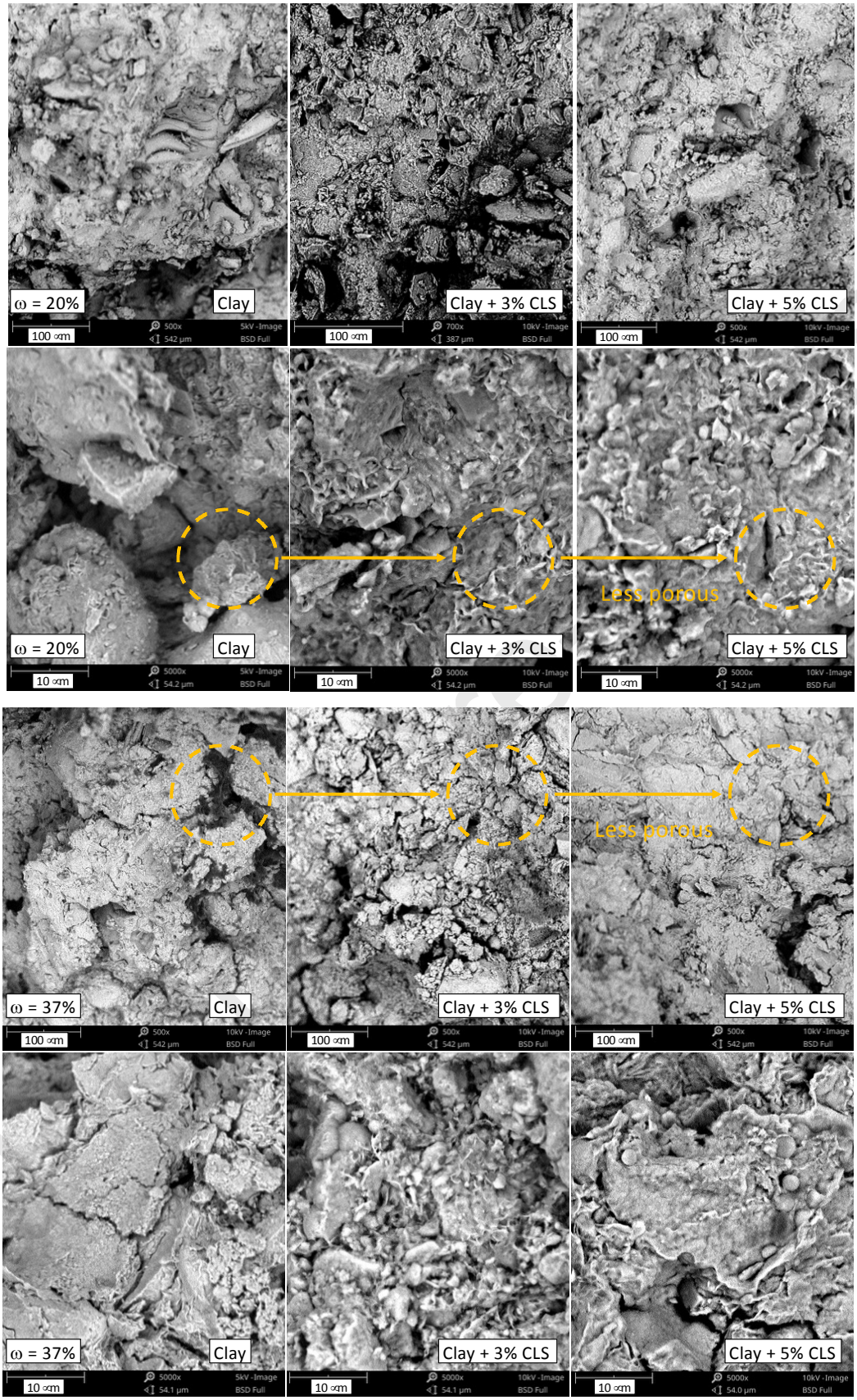

Figure 5: SEM for Clay, Clay + 3% CLS and, Clay + 3% CLS a) dry of optimum (ω = 20%) and b) wet of optimum (ω = 37%).

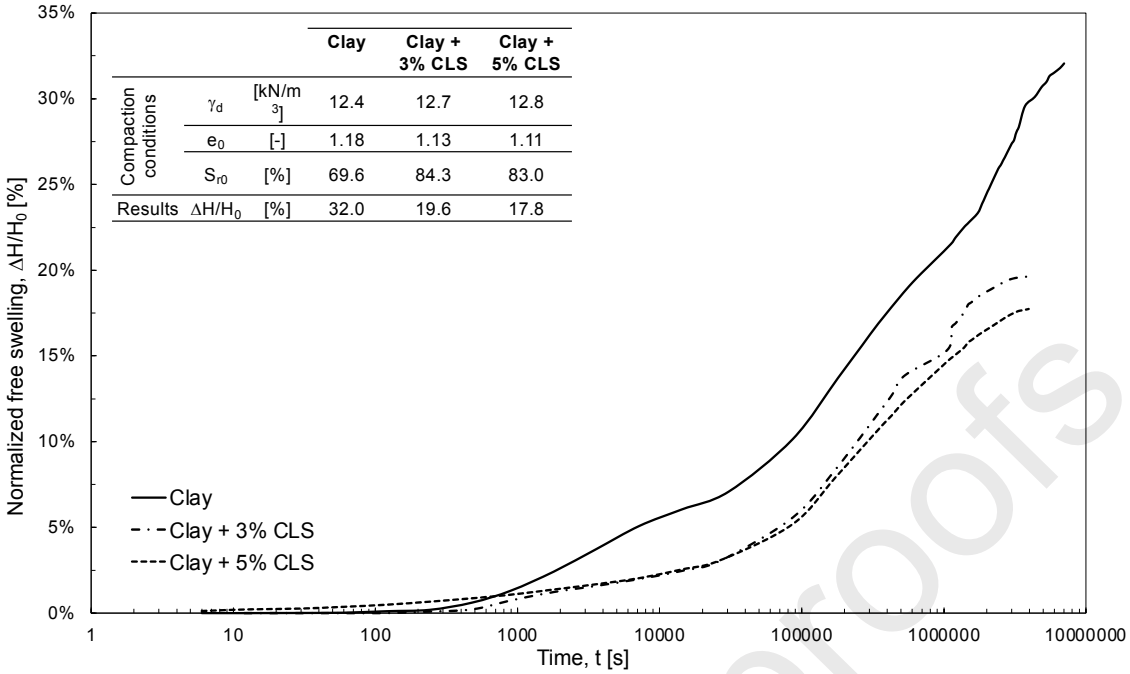

Figure 6: Free swell evolution with time for the three mixtures: Clay, Clay + 3% CLS and Clay + 5% CLS compacted samples at a given dry density (e = 1.18-1.23).

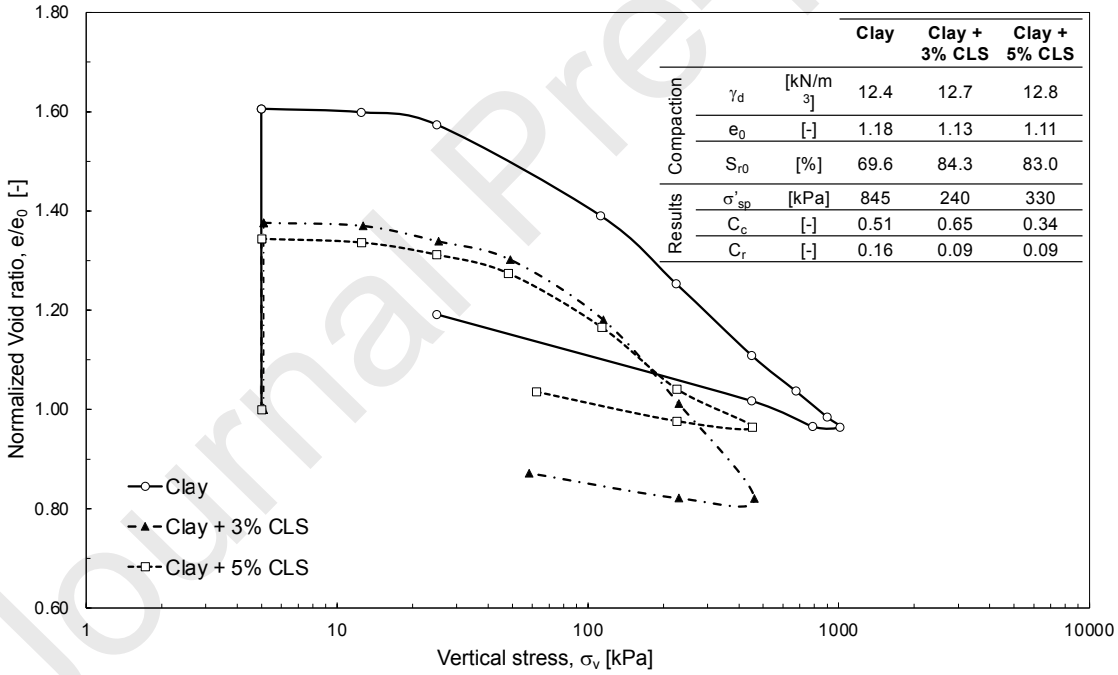

Figure 7: Results of swelling pressure and compressibility index obtained from evolution of the void ratio during free swell and Oedometer test for the three mixture: Clay, Clay + 3% CLS and Clay + 5% CLS compacted samples at a given dry density (e = 1.11-1.18).

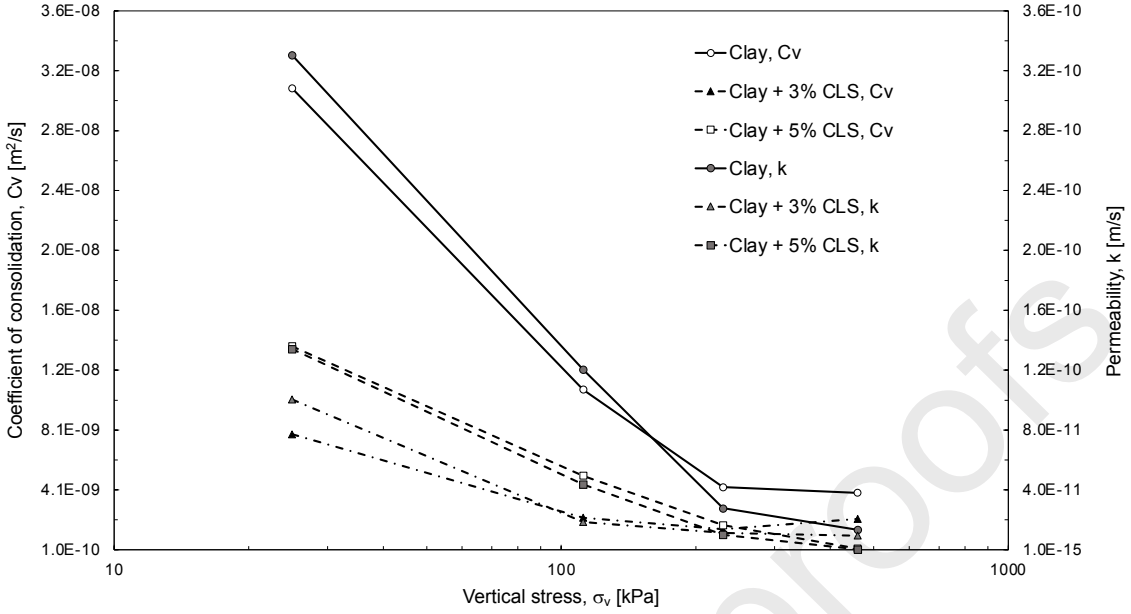

Figure 8: Evolution of consolidation and permeability parameter obtained from loading steps in Oedometer test for the three mixtures.

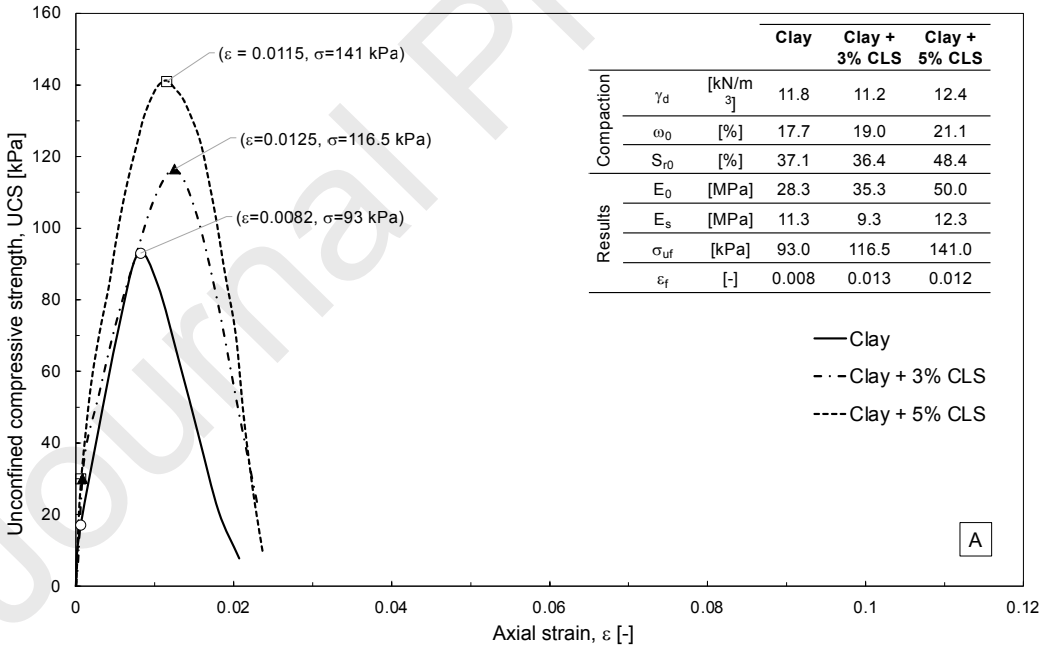

			Clay	Clay + 3% CLS	Clay + 5% CLS
Compaction	γ_d	[kN/m³]	11.8	11.2	12.4
	ω_0	[%]	17.7	19.0	21.1
	S_{r0}	[%]	37.1	36.4	48.4
Results	E_0	[MPa]	28.3	35.3	50.0
	E_s	[MPa]	11.3	9.3	12.3
	σ_{uf}	[kPa]	93.0	116.5	141.0
	ε_f	[-]	0.008	0.013	0.012

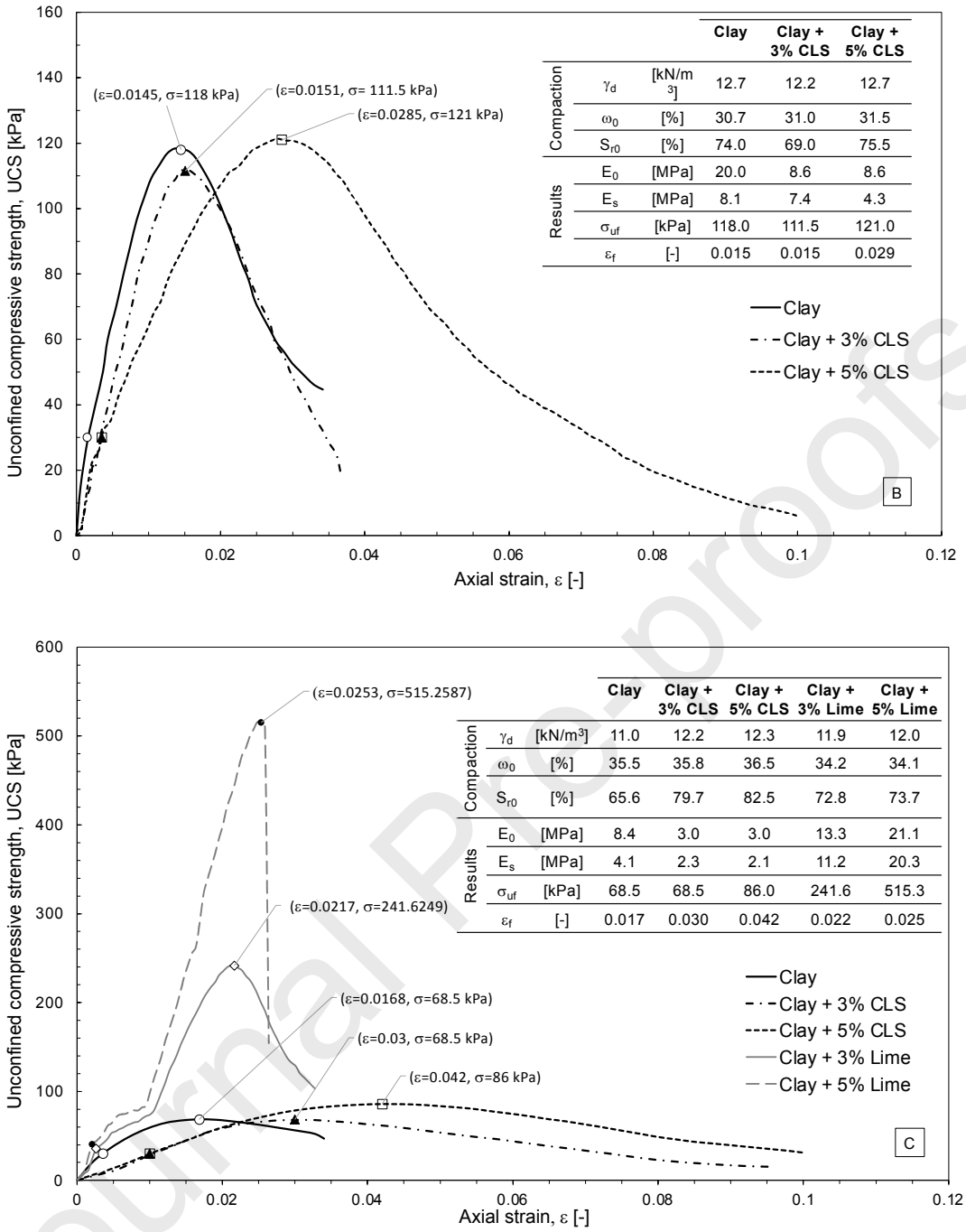

			Clay	Clay + 3% CLS	Clay + 5% CLS
Compaction	γ_d	[kN/m^3]	12.7	12.2	12.7
	ω_0	[%]	30.7	31.0	31.5
	S_{r0}	[%]	74.0	69.0	75.5
Results	E_0	[MPa]	20.0	8.6	8.6
	E_s	[MPa]	8.1	7.4	4.3
	σ_{uf}	[kPa]	118.0	111.5	121.0
	ε_f	[-]	0.015	0.015	0.029

			Clay	Clay + 3% CLS	Clay + 5% CLS	Clay + 3% Lime	Clay + 5% Lime
Compaction	γ_d	[kN/m^3]	11.0	12.2	12.3	11.9	12.0
	ω_0	[%]	35.5	35.8	36.5	34.2	34.1
	S_{r0}	[%]	65.6	79.7	82.5	72.8	73.7
Results	E_0	[MPa]	8.4	3.0	3.0	13.3	21.1
	E_s	[MPa]	4.1	2.3	2.1	11.2	20.3
	σ_{uf}	[kPa]	68.5	68.5	86.0	241.6	515.3
	ε_f	[-]	0.017	0.030	0.042	0.022	0.025

Figure 9: Unconfined Compressive test for the three mixtures: Clay, Clay + 3% CLS and Clay + 5% CLS compacted samples at a given dry density (γ_d = 11.0-12.3kN/m^3) and the moisture content: A) dry side of Optimum Proctor moisture content, B) optimum Proctor moisture content and C) wet side of Optimum Proctor moisture content and results for Clay + 3% Lime and Clay + 5% Lime.

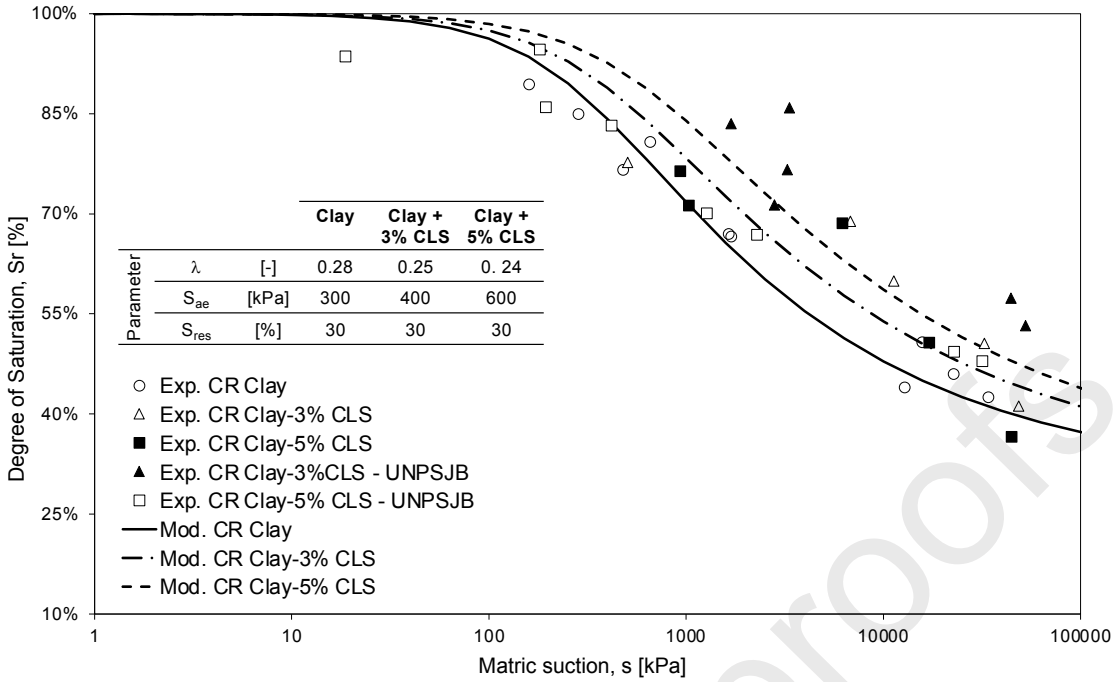

Figure 10: Relation of suction and degree of saturation using the filter paper technique and van Genuchten model for water retention curve for the three mixtures: Clay, Clay + 3% CLS and Clay + 5% CLS.

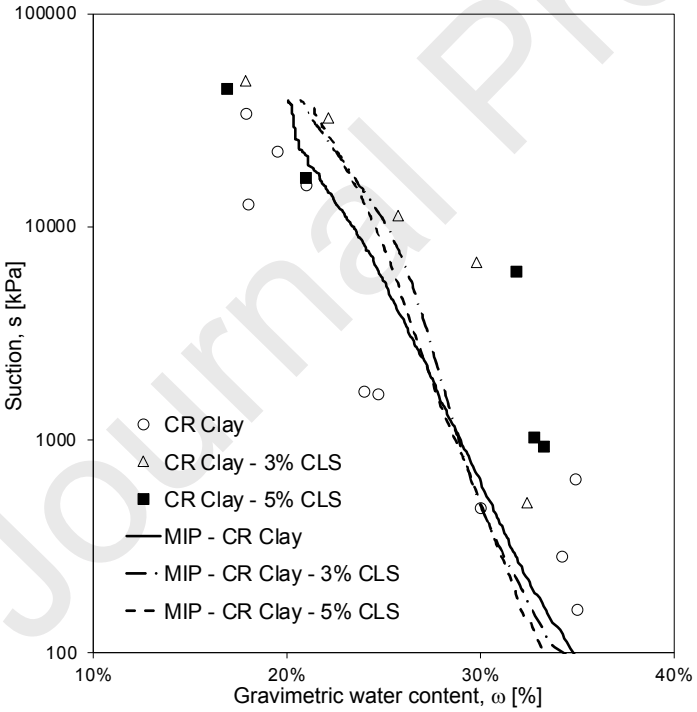

Figure 11: Comparison of gravimetric water content and degree of saturation using the filter paper technique with MIP results for the three mixtures: Clay, Clay + 3% CLS and Clay + 5% CLS.

Graphical Abstract

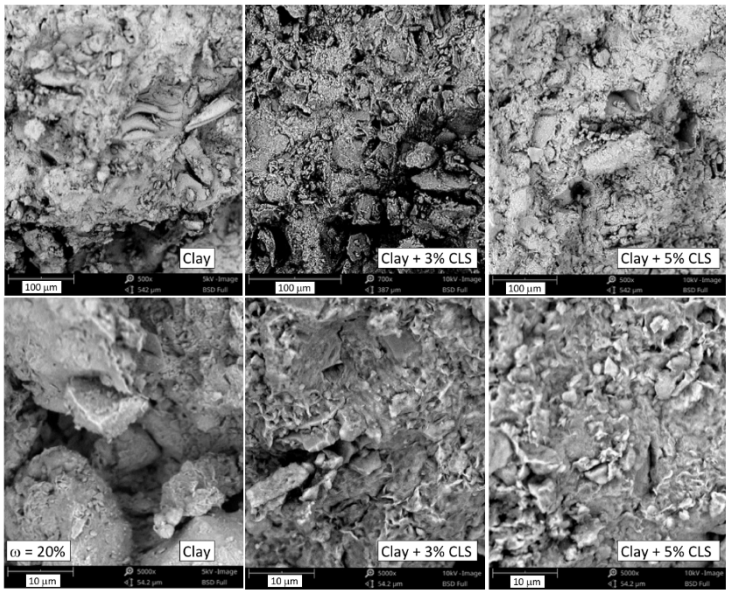

Highlights

This study analyses the efficiency of calcium lignosulfonate (CLS) as an expansible soil stabilization agent.

The evolution of micro and macro porosity of the clayey soil and CLS was analyzed with mercury intrusion porosimeter (MIP) and scanning electronic microscope (SEM).

Effect of the CLS on the hydro-mechanical behavior on compacted samples of Clay-CLS is evaluated.